Article ID: 1006-8775(2003) 02-0113-11

THE ANALYSIS ON THE STATISTICAL CHARACTER OF QUIKSCAT SCATTEROMETER WINDS AND STRONG WIND FREQUENCY USING REMOTE SENSOR DATA FROM QUIKSCAT

LIU Chun-xia (**刘春霞**)[1], HE Xi-cheng (**何溪澄**)[2]

(1. *Guangzhou Institute of Tropical and Marine Meteorology, CMA, Guangzhou* 510080 *China*; 2. *Guangdong Meteorological Bureau, Guangzhou* 510080 *China*)

ABSTRACT: The statistical character of QuikSCAT scatterometer winds is showed. And Monthly change and special distribution character of strong wind frequency and monthly wind fields in South China Sea is analyzed. It is shown in the result that the QuikSCAT scatterometer winds can be relied upon for the South China Sea; two winds, one the wintertime northeasterly and the other summertime southwesterly. The northeasterly centers at the Bashi Strait and Taiwam Strait and its secondary center and the maximum center of the southwesterly are in the central and southern South China Sea.

Key words: QuikSCAT scatterometer winds; strong wind frequency; wind fields

CLC number: P425.4.2 **Document code:** A

1 INTRODUCTION

Most of the conventional sea surface wind data are measurements from ships, buoys and islands, with coverage and spatial resolution far below the requirements of research and application. At present, due to limited understanding of physical processes and efficient exploitation of data, numerical prediction models have not been used as they should be, although routine procedures are able to give sea surface wind fields at the intervals of 6 hours. With the development of space remote sensing technique, satellite data are now playing a more important role owing to their large coverage, high temporal and spatial resolution and continuous observing capabilities. Sensors used to observe sea surface winds include microwave scatterometers, altigraphs and radiometers. Only the microwave scatterometers can give the output of sea surface wind vectors (wind direction and speed) under conditions of both find and cloudy sky while the other two only have wind speed at the sea surface. It is because of the advantage that the former instrument has been received so much recognition as it is.

The study on scatterometer data began in 1978 when it was first put to official use[1, 4]. The acquisition of the data from the European Remote-Sensing Satellite-1 (ERS-1) in 1992 and the European Remote-Sensing Satellite–2 (ERS-2) intensified its application in weather analysis, forecast and numerical prognosis[5-8]. For instance, by assimilation analysis of the wind field data achieved with scatterometers, weather analysis and forecast by numerical models have been improved for the Southern Hemisphere where conventional observations are scarce and far apart, tropical and extratropical cyclones have been better analyzed and predicted over the ocean of the Northern Hemisphere. On the other hand, the satellite data makes is possible to discover observational facts not available before and to trace wind trajectory. Operating for a short

Received date: 2003-06-24; **revised date:** 2003-1-19
Foundation item: Key Scientific Project of Guangdong province —Comprehensive application of satellite data in the monitoring and forecast of marine meteorology (99M05002G); Science and Technology Planning Project of Guangdong province —Research on pre-warning techniques for gale offshore Guangdong (2002B30906)
Biography: LIU Chun-xia (1968 –), female, native from Shangdu of Inner Mogolia Region, associate professor, undertaking the study of weather and climate.

duration on board the Japanese satellite, Advanced Earth Observing System (ADEOS), NASA's scatterometer (NSCAT) offers data that gives the application of scatterometer data a real big push[9-12]. Now the NSCAT data are used in the assimilation and analysis of sea surface data, air-sea interactions, and the tracking of tropical and extratropical cyclones. To make up the vacancy between ADEOS-I and ADEOS-II that was launched some time later, a polar satellite QuikSCAT was lifted into space by NASA in July 1999. Compared with other satellite-aboard scatterometers, the sensor, Seawind, can obtain wind vector data that is highly resolvable at 25 km × 25 km and has a larger swath of scanning (1800 km), covering 90% of the global ocean in a single day.

Wide application of the QuikSCAT has been reported abroad, ranging from data performance analysis to weather analysis and forecast. Besides, the data has been assimilated to routine numerical prediction models at the European Center for Medium-range Weather Forecast (ECMWF) and the National Centers of Environmental Prediction (NCEP) of the United States. A number of scientists are using the data in the research on climate analysis, air-sea interactions and sea ice. In the analysis of data performance, however, much effort is being paid to compare the scatterometer vector winds with global buoys and ships observations while there is hardly any work on comparison with island records. With the ERS-1 and ERS-2, Xie[18] studies the wind stress on the surface of the South China Sea and compares the difference among the observation means. Qi et al[19-20]. study the statistic features of altigraph wind speed and uses the data to analyze wind speed for all seasons and the monthly mean values for the South China Sea. There have not been any reports of domestic work on performance analysis of the QuikSCAT data. In the current work, 10-m wind field retrieved by the QuikSCAT scatterometer and the one measured on islands in the South China Sea are compared, error statistics determined and month-to-month wind field distribution and spatial distribution for the sea studied using the wind field data.

2 OPERATION PRINCIPLES AND QuickSCAT AND BRIEF ACCOUNT OF DATA

The scatterometer works by measuring the capability of backward scattering of microwave pulses transmitted to the earth surface to gauge the globe roughness. Over the ocean that covers 3/4 of the earth surface, the backward scattering waves are mainly composed of shortwave from the sea surface. Remote-sensing of sea surface wind is an idea that is based on the argument that minor perturbation of sea surface is in equilibrium state with local wind stress so that 10-m sea surface wind can be known by acquiring the backward scattering from it. From the scatterometer on board the QuikSCAT launched by NASA in 1999, Seawind, scans were made on the Ku band with "pencil-cluster" antenna cone over a swath of 1800 km, covering more than 90% of the global ocean daily.

The data used in the work is the third-level product processed by an air-sea team in the Jet Propulsion Laboratory (JPL), NASA. Its resolution is 0.5°×0.5°. To have a better analysis of the QuikSCAT data for different parts of the South China Sea, seven island stations are selected (Fig.1): Nan' ou (59324, 23 °26 ′ , 117 °02 ′), Dongsha (59792, 20°40 ′ , 116°43 ′), Weizhou Is. (59647, 21°02 ′ , 109°06 ′), Xisha (59981, 16°50 ′ , 112°20 ′), Shanhu Is. (16°32 ′ , 111°31 ′), Yongshu Reef (59995, 9°23 ′ , 112°53 ′) and Nansha (59997, 10°26 ′ , 114°22 ′). The data covers a length from September 1999 to December 2002. Optimized interpolated values are incorporated to the islands before making the comparison.

3 COMPARISON AND ANALYSIS OF QuikSCAT SCATTEROMETER WINDS AND ISLAND STATIONS MEASUREMENTS

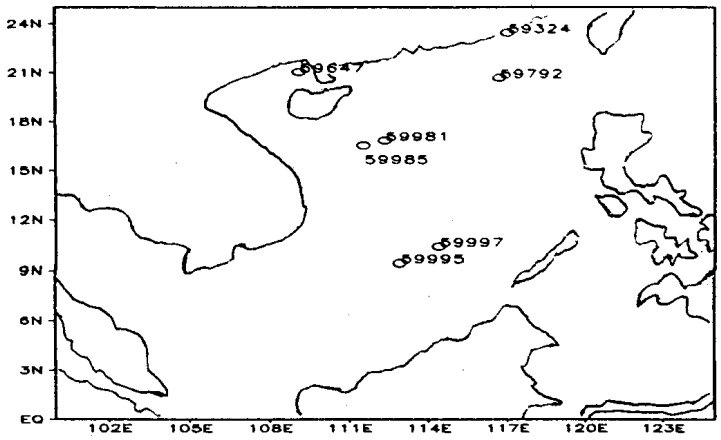

Fig.1 Distribution of observation stations

3.1 *Wind speed and direction*

Fig.2 compares the QuikSCAT wind speed and observed wind from the stations on the islands. The isolines in the figure stand for the frequency with which the wind speed appears. In other words, they are the frequency with which the QuikSCAT wind speed and observed wind from the island stations appear, in a way that resembles the scatter diagram. The interval of the isolines is 10 times and the diagonal in the figure indicates equality between the QuikSCAT wind speed and the observed wind. It is seen that the maximum frequency is more than 40 times and the location of the center is on the straight line linking two equal wind speed on the diagonal. It it then thought that the two speeds do not differ much from each other. Besides, for large frequencies, the axial straight lines are extending downward, showing part of the station wind speeds are smaller than the QuikSCAT one. Sought for the cause, it is considered the result from interpolation of the QuikSCAT wind speed to the latitude/longitude of the stations. The two wind speeds are being compared in different underlying surface of sea surface and islands and the larger roughness of the latter causes what we see in the comparison. Nevertheless, it is acceptable to use QuikSCAT wind speed to stand for sea surface wind speed less than 20 m/s.

With wind speed from different island stations and QuikSCAT is studied in more details (figure omitted), the error is the largest between them for Nan' ou Is. as the maximum frequency axis is the most far away from the diagonal. The distribution for Xisha and Nansha is similar to that of Fig.2, indicating significant influence of islands in vast ocean surface on wind

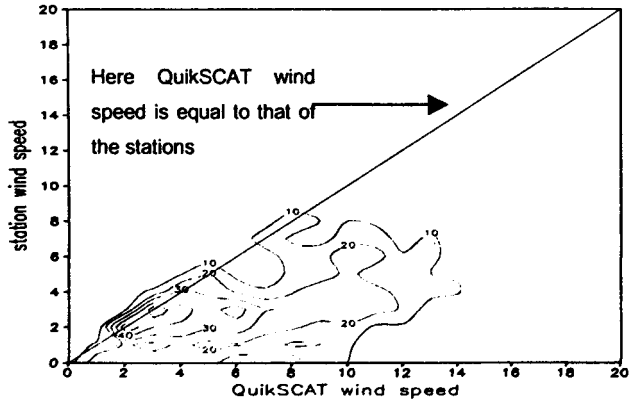

Fig.2 Comparison between the QuikSCAT wind speed (the abscissa) and stations wind speed (the ordinate). The isolines stand for the frequency with which wind speed appears.

measurements, which are made smaller than those with QuikSCAT. For Weizhou Is. in the Beibu Bay, however, the frequency maximum is on the diagonal and there is no secondary maximum center. It then has the minimum difference between the measurement types as compared to other stations. Results are less significant when the comparisons are made between reports from buoys and ships and QuikSCAT, it does show that the QuikSCAT wind speed can be relied on substantially for the South China Sea.

Fig.3 discusses how much the two types of wind speed resemble (differ from) each other. The isolines stand for the frequency with which wind direction appears and the diagonal represents the frequency with which both types of wind have the same direction. The figure shows that the centers of maximum for the appearance of wind direction frequency are well on the diagonal, indicating consistent direction in both of them. Although there is also a center of high frequency of wind direction for direction less than 60° with the QuikSCAT and at 360° with island measurement, the difference is about 60° from NE to N, showing that they do not differ much in wind direction. Studying the wind directions for all island stations and the QuikSCAT (figure omitted), we know that the largest frequency of wind direction for both types all distribute on the diagonal except for the station on the Nao' ou Is. It further shows that most of the observed wind direction agrees with the QuikSCAT wind direction. Locating near the coastline, the wind direction measured at Nan' ou and Weizhou Is. differs much from that of the QuikSCAT while the island measurements are well consistent with it. It then shows that the QuikSCAT wind direction is really reflecting the reality in areas close to the coast.

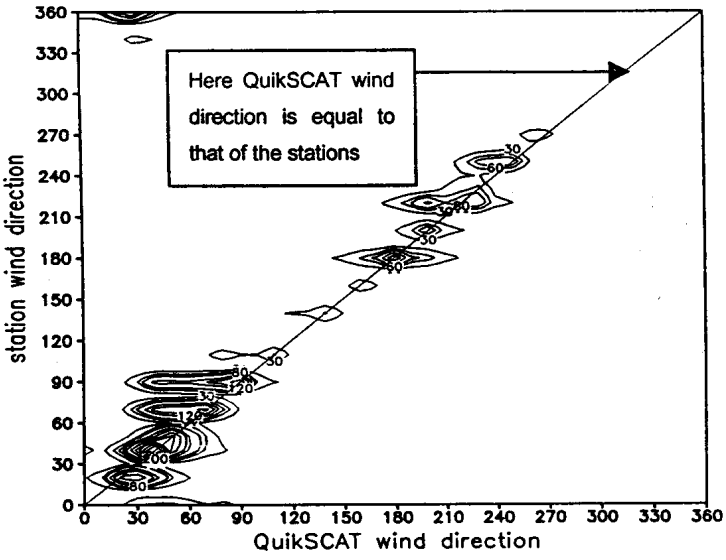

Fig.3 Same as Fig.2 but for wind direction (in unit of degree).

3.2 *Statistics of QuikSCAT wind direction and speed*

After the above comparison and analysis of wind speed and direction between the QuikSCAT and the seven island stations, we will analyze the statistics of the QuikSCAT wind direction and speed.

Tab.1 gives the statistics of vector wind comparison. The wind speed error between them amounts to 2.4 m/s, with the QuikSCAT wind speed generally higher than the island one, which is similar to the study above. The deviation wind direction is 26.7°, root-mean-square error in speed and direction is 3.6 m/s and 47.5°, respectively, and mean absolute error is 2.7 m/s and 30.5°, respectively. It is also found that the deviation, root-mean-square error and mean absolute error in wind speed is the maximum for Nan' ou, showing that the QuikSCAT wind speed is much

different from that taken at the station. It is also found that the wind speed error is relatively small for Yongshu Reef and Weizhou Is. near the Beiby Bay, though the sample size of the former statistics is much smaller. The difference is not large between the QuikSCAT and island measurements for Dongsha, Xisha and Nansha. For wind direction, stations with relatively small error include Dongsha, Yongshu and Nansha with mean absolute error less than 25° and deviation less than 20°. The larger error in wind direction appears in Nan'ou Is. where mean absolute error being as large as 49.1° and root-mean-error more than 60°. The findings agree with the preceding results with wind direction analysis.

Tab.1 Deviation, r.m.s error and absolute error of wind speed / direction by QuikSCAT and 7 island stations

Stations	WS deviation	WS r.m.s. error	WS m. Absolute erro	WD deviation	WD r.m.s. error	WD m. Absolute erro	Sample size
59324	3.8	5.1	4.1	-39.1	63.4	49.1	1951
59647	0.8	2.4	1.7	-23.1	53.8	36.4	1903
59792	0.9	3.2	2.3	-15.8	37.3	21.2	1684
59981	2.5	3.6	2.8	-33.1	41.8	29.2	1905
59985	2.7	3.5	2.9	-34.3	44.4	27.7	1896
59995	0.5	2.3	1.7	-19.0	41.6	23.2	906
59997	2.4	3.5	2.9	-16.5	39.7	21.1	1857
Sum of 7 stations	2.0	3.6	2.7	-26.7	47.5	30.5	12102

Tab.2 gives the ratio of correct percentage of wind speed over different sections, i.e. the percentages of island-observed winds and QuikSCAT scatterometer winds. It shows that the rate of correct wind speed is the highest at Yongshu Reef and Weizhou Is. near the Beibu Bay for the section between 0 m/s and 20 m/s while it is the lowest at Nan'ou Is. It is also found that the same two stations have higher rate of correct wind speed over the sections of 0 m/s – 5 m/s and 5 m/s – 10 m/s, appearing more than 60% of the opportunity. The correct rate is all over 60% at Dongsha, Xisha and Yongshu and compares favorably with other sections of wind speed with the lowest rate over 50%. The correct rate is the lowest for the section from 15 m/s to 20 m/s and even zero for the Weizhou Is. and Dongsha. For all of the seven island stations, the rate is the highest for the section 10 m/s – 15 m/s but the lowest 15 m/s – 20 m/s. It shows that the QuikSCAT is the lowest for wind speed more than 15 m/s.

Tab.2 Sectional percentage of correct wind speed by QuikSCAT

stations	0—5 m/s	5—10 m/s	10—15 m/s	15—20 m/s	0—20 m/s
59324	39.3	42.8	51.5		40.2
59647	66.4	70.3	58.8	0.0	67.1
59792	55.0	54.2	61.9	0.0	54.2
59981	44.5	53.6	63.6		46.8
59985	51.3	32.7	50.0		48.4
59995	79.5	83.1	68.5	38.9	78.7
59997	47.8	50.2	54.3		48.3
Sums of 7 stations	51.3	56.6	62.0	11.9	52.8

From the analysis, we note that (1) of the seven stations the error of QuikSCAT wind speed and direction is the largest at Nan'ou; (2) the error of wind speed is relatively small but that of wind direction relatively large at the Weizhou Is.; (3) wind speed is slightly smaller at Dongsha,

Xisha, Nansha Is. than the QuikSCAT wind speed, and so is the error in wind direction; (4) it is generally the case that vector winds from the QuikSCAT scatterometer is applicable for the South China Sea, though care should be taken as to the correctness of wind direction by QuikSCAT when it comes to the coastal region. Cautions should also be taken to note the effect of the east Guangdong coast on the QuikSCAT wind speed.

4 ANALYSIS OF STRONG WINDS OVER THE SOUTH CHINA SEA

4.1 *Influence on temperature fields*

To study the wind field and distribution of strong winds over the South China Sea, a spatial description of monthly mean wind field as depicted by QuikSCAT for Jan. Mar. May, Jul. Sept. And Nov. is given in Fig.4. Figures for the remaining months are omitted. It shows that the northeasterly wind prevails in Jan. and the maximum mean wind is greater than 9 m/s, with two high-value centers respectively locating at 110°E, 11°N and Bashi Strait region and Taiwan Strait in the northeastern South China Sea. The centers remain strong until February with the maximum as much as 10 m/s or more. The two centers are still there in Marhc though with the maximum decreasing to 7 m/s. In Apr., the mean maximum wind speed is only 4 m/s – 5 m/s and the centers are poorly defined. It is found that there is a center of wind speed in the Beibu Bay to the southwest of the Hainan Is with the maximum at 4 m/s. In May, the maximum wind speed is moderate but with the distribution very different from Apr., with the high-value center almost unseen in the northeastern part of the sea while the other at 110°E, 11°N is still there, only that the easterly wind seen in Apr. has been replaced by the southwesterly, indicating that it is formed because of the onset of the southwest monsoon. In Jun. – Sept., the latter center is maintaining, varying from 6.5 m/s in Jun., through 9 m/s in Aug., till 5 m/s in Sept. The southwesterly is a dominant wind for the entire South China Sea in Jun. – Aug. until Sept. when the northeasterly appears in the northern part of the sea, which gradually advances southward, covering the entire region in Nov. At the time, the southwest maximum begins to disappear in the central and southern part of the sea while the northeast maximum becomes well-defined over the Bashi Strait and Taiwan Strait. The distribution of Nov. and Dec. are similar to that of Jan. – Mar. with two centers of the northeasterly and the northern one significantly larger than the southern one. They both reach the maximum in Dec., 11 m/s for the northern and 10 m/s for the southern.

From the analysis above, we discover that the northeasterly becomes the dominant mean wind from autumn in the northeastern part of the sea. It then keeps increasing till winter and maintaining to Mar., with the monthly mean wind speed reaching the maximum in Dec. The center of northeasterly wind does not disappear until Apr. and reappears in Sept. and its center is poorly defined until Nov. Strong winds on the northeast - southwest axis in northern South China Sea are decreasing. It is now clear that the center of strong winds in the region reflects the effect of the winter monsoon and the channeling effect of the straits make the wind stronger. The center in the central and southern South China Sea is different from the one in the northern part of it. Apart from Apr. and Oct., the northern center is the maximum center of northeasterly from Nov. to Mar. with the monthly mean speed maximum at 10 m/s from Dec. to Jan. with the onset of the southwest monsoon, the high-value center changes from the northeasterly to southwesterly and begins expanding east and north in Jun. with the maximum in Aug. and monthly mean maximum wind speed at 9 m/s. The center of strong winds in the central and southern part of the sea reflect the advancement of winter and summer monsoon in central South China Sea.

With the GEOSAT altigraph, Qi et al. give the distribution of wind speed in four seasons in the South China Sea. They think that there are two wind speed areas in spring (Feb. – Apr.) and autumn (Aug. – Oct.), one being a tongue-shaped high-value area decreasing from northeast to southwest in northeastern South China Sea and a secondary speed area at 110°E, 11°N.

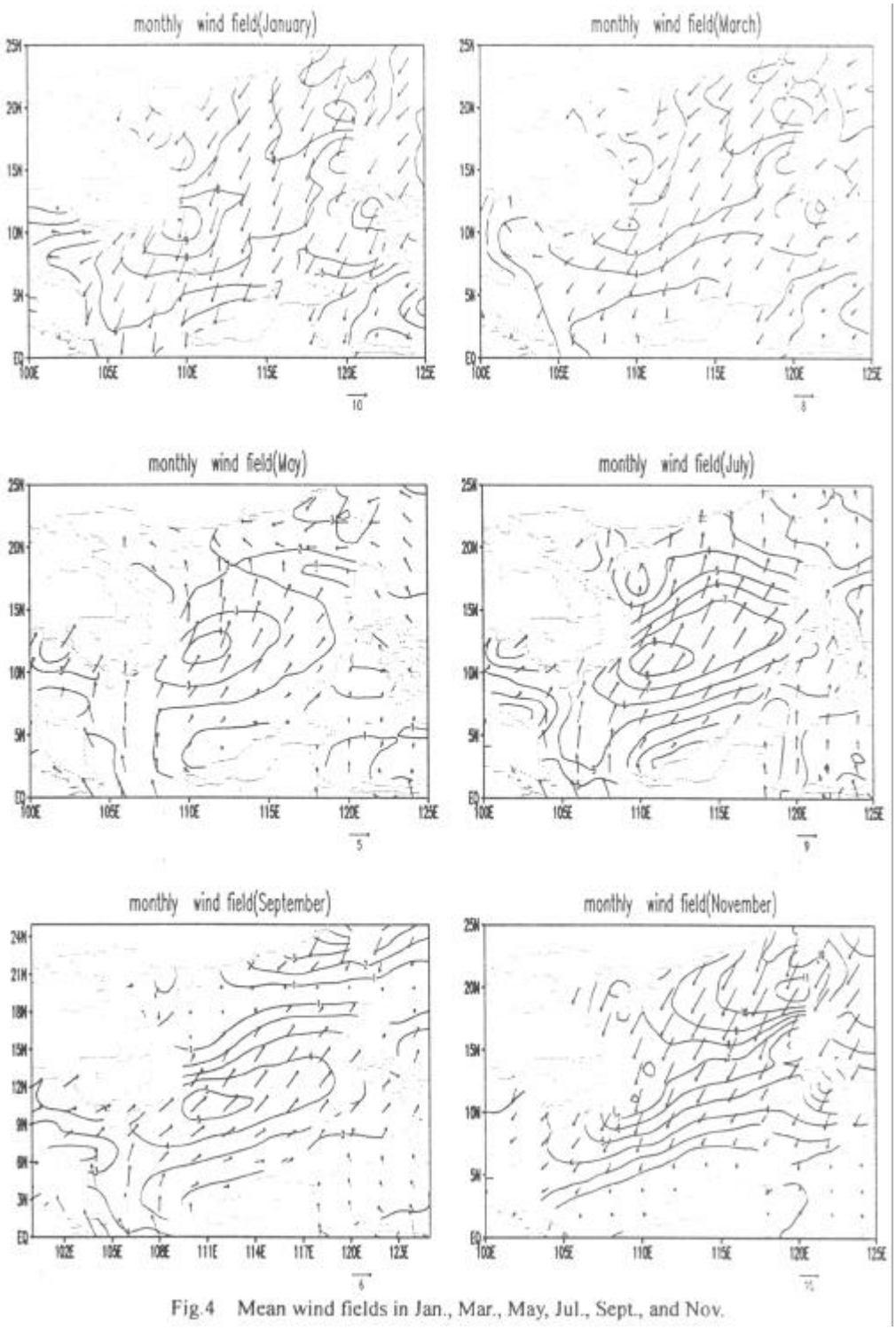

Fig.4 Mean wind fields in Jan., Mar., May, Jul., Sept., and Nov.

Examining the analysis of monthly wind field, we find that Feb. and Oct. are the months that mark with such characteristics. Qi et al. point out that the winter (Nov. – Jan.) is marked by maximum wind speed in northeastern waters of the sea, being over 10 m/s over the Bashi Strait

and decreasing along a NE – SW axis. It is 9 m/s in the maximum area of the secondary wind speed. The distribution is the same as that by the QuikSCAT for Nov. – Jan., without much difference between the two speed maxima. For the altigraph measurement, the secondary summer (May – Jul.) wind speed center changes to the maximum center with the value more than 8 m/s. Correspondingly, the QuikSCAT distribution has similar distribution as the altigraph in May – Jul. It shows that the two types of remote-sending data have the consistent distribution of sea surface wind. Additionally, when we compare the QuikSCAT scatterometter wind field with the altigraph sea surface winds, we could find two prevailing wind directions (NE and SW) in individual months over the sea and their advancement stages as well as the distribution of wind speed. The NE wind begins to move south in Sept. from the northern part of the sea and arrives at 3°N in Nov. In Apr., NE wind is replaced by E wind over most of the South China Sea. From south to north, the SW wind takes control from May and the NE wind begins advancing from Sept. The whole process shows how the NE and SW monsoon affect the South China Sea.

4.2 *Distribution of strong winds frequency in the South China Sea*

From the comparison of wind direction and speed between the islands stations and QuikSCAT, we think that the satellite scatterometer data can well describe winds above Force 6 ($\geq$ 10.8 m/s) but work less satisfactorily for winds above 15 m/s. In view of it, frequencies with which strong winds higher than Force 6 appear are discussed here. Studying the monthly mean frequency for strong winds (Fig.5), we know that there is a frequency center of NE gale near the Bashi Strait and over the Taiwan Strait from Oct. (autumn) to Mar. (early spring), with the maximum of 20 days in Dec. The center has a much-decreased frequency in Apr., and it is only 4 days from May to Sept., possibly caused by tropical cyclones. Similar to the monthly mean wind field, there is a center of strong winds frequency near 110°E, 11°N, which appears in Nov. – Mar. and Jun. – Aug. The NE gale prevails for more than 10 days in Nov. – Feb., having the maximum in Dec. The freqUency for SW gale increases from 6 days in Jun. to 12 days in Aug. In contrast, there are at most 2 days in which strong winds prevail in the region in Apr., May, Sept., and Oct. Furthermore, the axis for the maximum gale frequency for the whole sea is in the direction NE – SW in the autumn and winter; for the northern part of the sea, the frequency is much higher for the NE gale to appear than for the SW gale and the autumn and winter is a time that marks much higher frequency of strong winds as compared with the spring and summer (Apr. – Aug.). The latter is mainly affected by strong winds from the tropical cyclone, with the frequency no more than 6 days. In addition to the areas above, gale weather can also appear in the Beibu Bay with a frequency under 8 days, much smaller than the northeastern South China Sea.

Studying the centers of gale frequency and maximum wind field, we know that the former has a highly consistent variation with the monthly mean wind speed in terms of seasonal changes, and so does the location of the centers. The northeastern part of the sea, including the Taiwan Strait, Bashi Strait, witnesses the largest frequency of NE gale, agreeing with previous work. For the northern part of the sea, however, the gale frequency decreases from east to west, with the number of days having strong winds much more in the eastern than in the western part. It should be noted that the center of gale and the central location of the frequency center over the central and southern part of the sea are just close to the ascending ocean current, which is a hot topic in the oceanographic community. It may be one of the regions where significant local air-sea interactions take place. The center well reflects the effect of the winter and summer monsoon on the South China Sea (Fig.6). It shows monthly mean wind speed and monthly gale frequency at 110°E, 11°N. Interannual variations exist in the center values but we cannot study their laws due to limited length of data. The figure shows consistence between gale frequency and mean wind speed.

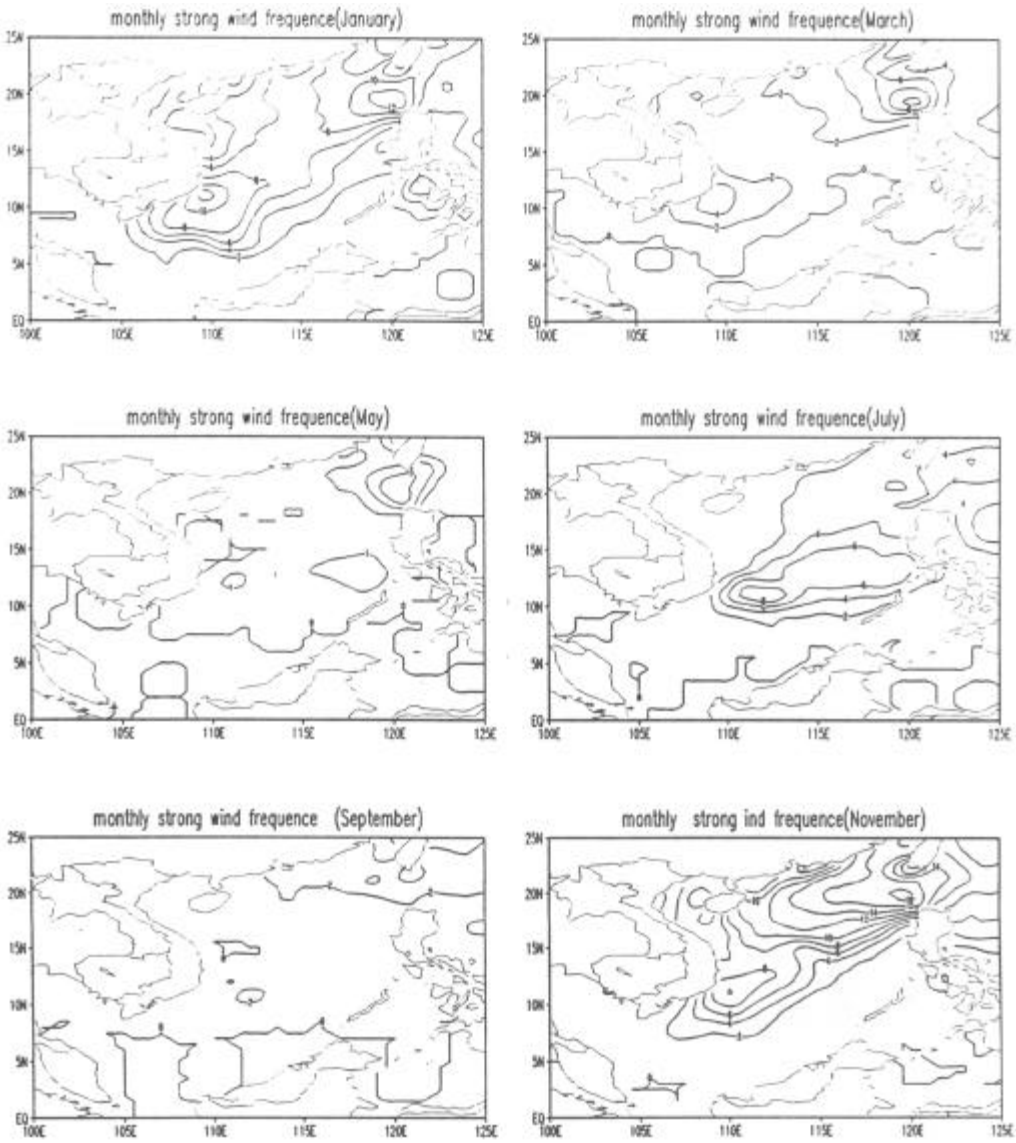

Fig.5 Frequency with which winds above Force 6 appear in Jan., Mar., May, Jul., Sept., Nov.

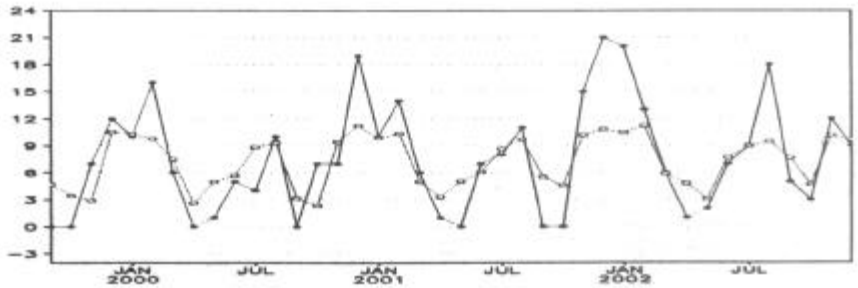

Fig.6 Time series of wind speed (dashed line) and time series of frequency with which winds above Force 6 appear (solid line) at 110°E, 11°N. The time spans from Sept. 1999 to Dec. 2002.

5 CONCLUDING REMARKS

a. Analyzing island station wind speed, direction and QuikSCAT vector wind, we know that the probability is the maximum for them to be equal. It is shown that the QuikSCAT vector wind is highly reliable for the South China Sea, but attention should be given to the effect of coastline on the QuikSCAT scatterometer wind direction measurements.

b. As shown in the error statistics, the deviation of wind speed is 2.4 m/s, with the QuikSCAT scatterometer wind speed generally higher than that taken by island stations and the deviation is 26.7° in wind direction; the root-mean-square for wind speed and direction is 3.6 m/s and 47.5°, respectively; the mean absolute error for both speed and direction is 2.7 m/s and 30.5°, respectively.

c. The correct rate is the highest for the section from 10 m/s to 15 m/s but the lowest from 15 m/s to 20 m/s, while it is over 50% for the section from 0 m/ to 10 m/s.

d. There are two areas of strong winds as revealed by the analysis of monthly mean wind fields. The first is in the northeastern South China Sea that includes the Bashi Strait and Taiwan Strait, which appears during the period of NE wind maintenance. The center of high winds stays on from autumn to Mar. (spring), with the maximum of wind speed in Dec. The second one is in the central and southern part of the sea, which witnesses prevailing northeasterly wind from Nov. to Mar. but prevailing southwesterly wind from May to Sept. The distribution of high-value centers by QuikSCAT is similar to that of the South China Sea wind speed achieved by Qi et al. with the altigraph.

e. As shown in the analysis of frequency for Force 6 wind in individual months, the centers of strong wind frequency exist in the Taiwan Strait, Bashi Strait and the central and southern South China Sea, corresponding to the centers of high wind speed values. For the northern part of the sea, however, the center of maximum strong wind frequency appears in the months when the winter monsoon prevails, with the frequency decreasing from east to west. For the central and southern part of the sea, the center of maximum strong wind appears in the season when the winter monsoon (Oct., Nov., Dec., Jan. – Mar.) and the summer monsoon (May – Aug.) prevail. Strong winds do occur in the Beibu Bay but with much smaller intensity. For the whole of the sea, the frequency for the NE gale to appear over the coarse of the year is much higher than that for the SW gale. It is then a sign that the cold air is the main weather system that affects the appearance of strong wind in the sea. The role of SW gale cannot be neglected either, because the ascending ocean current is located around the area 110°E, 11°N from which ascending current occurs. It can be viewed as the key region for potential local air-sea interactions.

Acknowledgements: Mr. CAO Chao-xiong, who works at the Institute of Tropical and Marine Meteorology, CMA, Guangzhou, has translated the paper into English.

REFERENCES:

[1] WURTELE MG, WICESHYN P M, PETEGHER YCH, et al. Wind direction alias removal studies of SEASAT scatterometer-derived wind fields [J]. *J Geophys Res*, 1982, **87**: 3365-3377.

[2] YU T W, MCPHERSON R D. Global data assimilation experiments with scatterometer winds from SEASAT-A [J]. *Monthly Weather Review*, 1984, **112**: 368-376.

[3] CHEN Lie-ting. Effect of zonal difference of sea surface temperature anomalies in the Arabian Sea and the South China Sea on summer rainfall over the Yangtze River [J]. *Scientia Atmospherica Sinica*, 1991, **15**: 33-42. PIERSON W J, SYLVESTER W B, DONELON M A. Aspects of the determination of winds by means of scatterometry and of the utilization of vector wind data for meteorological forecasts [J]. *Journal of Geophyics Research*, 1986, **91**: 2263-2272.

[4] PIERSON W J. Probabilities and statistics for backscatter estimates obtained by a scatterometer [J]. *Journal of Geophyics Research*, 1989, **94**: 9743-9759.

[5] HOFFMAN R N. A preliminary study of the impact of the ERS1 C-band scatterometer wind data on the ECWMF global data assimilation system[J]. *Journal of Geophyics Research*, 1993, **98**: 10233-10244.
[6] HSU C S, LIU W T. Wind and pressure fields near tropical cyclone Oliver derived from scatterometer observations[J]. *Journal of Geophyics Research*, 1996, **101**: 17021-17027.
[7] SCHMULLIUS C C. Monitoring Siberian forecast and agriculture with the ERS-1 wind scatterometer [J]. *IEEE Trans Geosci Remote Sens*，1997, **35**: 1364-1366.
[8] ISAKSEN L, STOFFELEN A. ERS scatterometer wind data impact on ECWMF's tropical cyclone forecasts [J]. *IEEE Trans.Geosci Sens*, 2000, **38**: 1885-1892.
[9] ATLAS R, BLOOM S C, HOFFMAN R N, at el. Geophysical validation of NSCAT winds using atmospheric data and analyses [J]. *Journal of Geophyics Research*, 1999, **104**: 11405-11424.
[10] CHANG C P, LIN S C, LIOU C S, et al. Qn experiment using NSCAT winds in numerical predication of tropical mesoscale rainfall systems under the influence of terrain [J]. *Geophys Res Lett*, 1999, **26**: 311-314.
[11] CHU P C, LU S, LIU W T. Uncertainty of South China prediction using NSCAT and NCEP winds during tropical storm Ernie 1996[J]. *Journal of Geophyics Research*, 1999, **104**: 11273-11289.
[12] LIU W T, TANG W, HU H. Spaceborne sensors observe various effects of anomalous winds on sea surface temperatures in the Pacific Ocean [J]. *Eos Trans AGU*, 1998, **79**: 249-252.
[13] FIGA J, STOFFELEN A. On the Assimilation of Ku-band scatterometer winds for weather analysis and forecasting [J]. *IEEE Trans Geosci Remote Sens*, 2000, **38**: 1893-1902.
[14] LIU W T, HU J, YUEH S. Interplay between wind and rain observed in hurricane floyd [J]. *Eos Trans AGU*, 2000, **81**: 253-257.
[15] LIU W T, XIE X, POLITO P S, at el. Atmosphere manifestation of tropical instability wave observed by QuikSCAT and tropical rain measuring missions [J]. *Geophys Res Lett*, 2000, **27**: 2545-2548.
[16] ATLAS R, HOFFMAN R N, LEIDNER S M, at el. The effects of marine winds from Scatterometer data on weather analysis and forecasting [J]. *Bull Amer Meteor Soc*, 2001, **82**: 1965-1990.
[17] LIU W T. Progress in scatterometer application [J]. *J Oceanography*, 2002, **58**: 121-136.
[18] XIE Qiang, WANG Dong-xiao, WANG Wei-qiong et al. Comparison among four kinds of data of sea surface wind stress in South China Sea [J]. *Journal of Tropical Oceanography*. 2001, **20** (1): 91-100.
[19] QI Yi-quan, SHI Ping, MAO Qing-wen. Seasonal characteristics of the sea surface wind speeds in the South China Sea by remote sensing [J]. *Tropic Oceanology*, 1996, **15** (1): 68-73.
[20] QI Yi-quan, SHI Ping. Analysis of monthly average distribution characteristics of sea surface wind and wave in South China Sea using altimetric data [J]. *Tropic Oceanology*, 1999, **18** (1): 68-73.